

Imidazole derivative as novel effective inhibitor of mild steel corrosion in aqueous sulphuric acid

Nnenna Winifred Odozi¹, Jonathan Oyebamiji Babalola¹, Ekemini Bassey Ituen^{2*}, Abiodun Omokehinde Eseola³

¹Department of Chemistry, University of Ibadan, Ibadan, Oyo State, Nigeria

²Department of Chemistry, University of Uyo, Uyo, Akwa Ibom State, Nigeria

³Department of Chemistry, Redeemers University, Ede, Ogun State, Nigeria

Email address:

ebituen@gmail.com (E. B. Ituen)

To cite this article:

Nnenna Winifred Odozi, Jonathan Oyebamiji Babalola, Ekemini Bassey Ituen, Abiodun Omokehinde Eseola. Imidazole Derivative as Novel Effective Inhibitor of Mild Steel Corrosion in Aqueous Sulphuric Acid. *American Journal of Physical Chemistry*. Special Issue: Paradigm Shift in Corrosion Studies and Elucidation of Mechanism of Corrosion Inhibition. Vol. 4, No. 1-1, 2015, pp. 1-9.
doi: 10.11648/j.ajpc.s.2015040101.11

Abstract: Corrosion behavior of mild steel immersed in 0.5 M H₂SO₄ and corrosion inhibition in the presence of different concentrations of 2,4-di-tert-butyl-6-(1h-phenantro[9,10-d]imidazol-2-yl) phenol (PIP) was investigated using weight loss and hydrogen evolution techniques at 303 – 333 K. The results indicate a maximum inhibition efficiency of 68.45% in the presence of 10 x 10⁻⁵ M PIP at 303 K. The inhibitory action of PIP in the acid solution is best described by Temkin adsorption isotherm. The Arrhenius and transition state equations are used to calculate activation parameters and the mechanism of physical adsorption is proposed for PIP from the values of E_a and ΔG^{*}_{ads} obtained. Thermodynamic studies indicate that the adsorption of PIP to the metal surface is spontaneous. Quantum chemical calculations using DFT is used to calculate some electronic properties of the molecule in order to ascertain any correlation between the inhibitive effect and molecular structure of the molecule PIP. PIP protected the mild steel against corrosion in the acid medium at the studied temperatures by virtue of adsorption. The corrosion rate increased with temperature both in the absence and presence of the inhibitor, but the increase was lesser in the presence of the inhibitor compared to that of the free acid solution. The inhibition efficiency increased with increase in concentration of the inhibitors.

Keywords: Adsorption Isotherm, Corrosion Inhibitors, Density Functional Theory (DFT), Mild Steel, Physical Adsorption, Imidazole

1. Introduction

Imidazole is an organic compound with the formula C₃H₄N₂. It is an aromatic, heterocyclic compound, a diazole usually classified as an alkaloid. This ring system is present in important biological building blocks such as histidine, and the related hormone histamine. Imidazole can serve as a base and as a weak acid. Antifungal drugs and nitroimidazoles contain the imidazole ring [1]. Synthetic imidazoles have been used as medications such as antifungal, fungicides, antiprotozoal, and antihypertensive medications. They are also part of the theophylline molecule, found in tealeaves and coffee beans, which stimulate the central nervous system. It is present in the anticancer medication, mercaptopurine, which combats leukemia by interfering with DNA activities.

Recently, imidazoles and its derivatives have been used as efficient and effective corrosion inhibitors of metals in different aggressive media. Corrosion inhibitors are organic compounds containing polar functionalities such as oxygen, nitrogen, sulphur, and phosphorus in their molecular structure and are capable of retarding the dissolution of metals in the aqueous aggressive medium via adsorption on to metal surface, forming films, thereby shielding the metal from the corrosive agents present in solution [2].

The presence of these heteroatoms in the inhibitor molecular structure makes possible its adsorption by coordinate type linkage through transfer of lone pairs of electrons from the heteroatoms to the steel surface, resulting in a stable chelate ring with ferrous ions [3]. The aim of this work therefore is to explore the use of PIP as corrosion

inhibitor for mild steel surface in sulphuric acid solution using gravimetric method. The effect of temperature on corrosion and inhibition processes are thoroughly assessed and discussed. Kinetic and thermodynamic parameters were also calculated and discussed. The quantum chemical study using density functional theory was further employed to provide additional insight into the mechanism of inhibitory action.

2. Experimental Method

2.1. Materials

Mild steel (thickness = 0.46mm) used in the study with composition (wt. %): 0.13 C, 0.18 Si, 0.39 Mn, 0.60 P, 0.04 S, 0.025 Cu, and bal Fe), were mechanically cut into 4.0 cm × 4.0 cm × 0.046 cm dimensions, washed in absolute ethanol and acetone, dried at room temperature and stored in a moisture free desiccator before their use in corrosion studies [4]. The inhibitor was synthesized and fully characterized according to recent report [5]. As presented in Figure 1 (b), the ^1H nmr spectra of the inhibitor shows it is spectroscopically pure and was used without further purification. The concentration range for the inhibitor was 2×10^{-5} to 10×10^{-5} M. Fig. 1(a) shows the molecular structure of PIP.

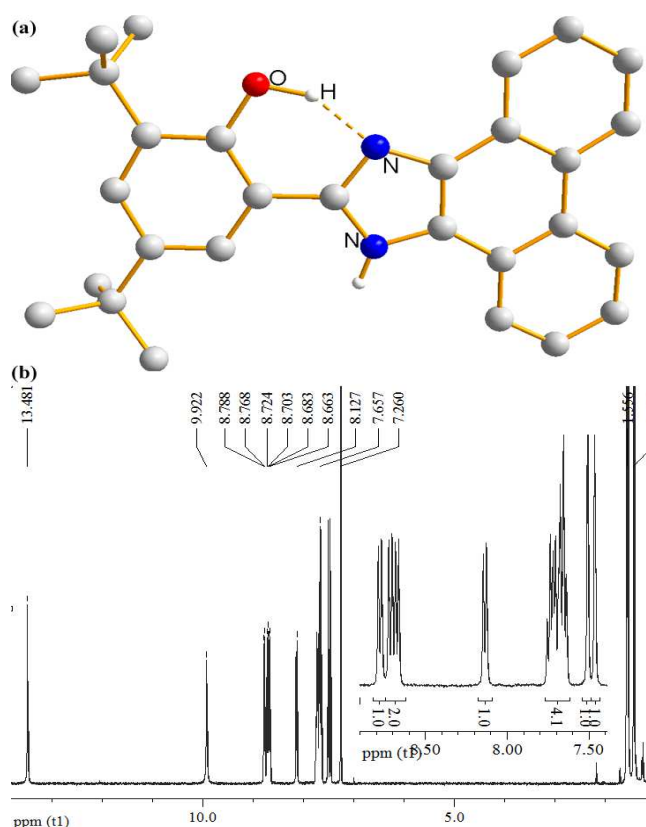


Fig 1. (a) Perspective view and (b) ^1H nmr spectra of 2,4-di-tert-butyl-6-(1H-phenantro[9,10-d]imidazol-2-yl)phenol (PIP)

2.2. Solutions

The corrosive agent was H_2SO_4 from BDH and the concentration prepared and used was 0.5 M. The PIP solution

was prepared by dissolving 0.0422g of an accurately weighed PIP in about 5cm^3 of methanol, stirred thoroughly until complete dissolution. The solution was then transferred into a 1000 cm^3 volumetric flask containing the 0.5 M sulphuric acid, and then made up to mark with the acid solution to obtain the highest concentration (10×10^{-5} M) of the inhibitor. Other lower concentrations of the inhibitor solution were prepared from the popular dilution principle. All preparations were made in double de-ionized water.

2.3. Weight Loss Method

The weight loss measurement was conducted under total immersion using 250 mL capacity beakers containing about 20mL of the test solution. The pre-weighed mild steel sheets were immersed in the beaker containing the test solutions. The coupons were retrieved at 2 hours interval progressively for 10 hours, washed thoroughly in 20% NaOH solution containing 200 g/L of zinc dust (ASTM G1-72, 1990) with thistle brush, rinsed convincingly in distilled water, cleaned, dried in acetone, and re-weighed using a FA2104A digital weighing balance with sensitivity $\pm 0.0001\text{g}$. The difference in the weight of the mild steel coupons before and after immersion in different test solutions was recorded as the weight loss. This was repeated at different temperatures. To ensure reproducibility, experiments were carried out in triplicates and the standard deviation values among parallel triplicate experiments were found to be smaller than 3%, indicating reliability and reproducibility.

The corrosion rate was calculated from the weight loss data using the relationship [6]:

$$v = (m_1 - m_2)/AT \quad (1)$$

where v ($\text{mgcm}^{-2}\text{h}^{-1}$) is the corrosion rate, m_1 and m_2 (g) are the weights before and after immersion respectively in the test solutions, A (cm^2) is the surface area of the coupons and T (s) is the immersion time. The inhibition efficiency (%) was then computed from the following equation [7]:

$$\%I = 100 (v_b - v_i)/v_b \quad (2)$$

where v_b and v_i are the corrosion rates in the absence and presence of the inhibitor respectively.

2.4. Hydrogen Evolution Technique

A gasometric assembly was used for this measurement. Detailed description of the assembly has been reported elsewhere [8]. About 100 cm^3 of the test solutions was used and the corrosion process monitored by careful measurement of the volume of hydrogen gas evolved at fixed intervals both for the uninhibited and the inhibited solutions at 303 – 333 K. The volume of hydrogen gas evolved was used to calculate the corrosion rate of the mild steel which (equation 3) is a function of the rate of hydrogen gas evolution.

$$R_H = (V_t - V_i)/(T_t - T_i) \quad (3)$$

where V_t and V_i are the volumes of hydrogen evolved at time T_t and T_i respectively. The inhibition efficiency (%) I was

computed using the equation 4 below:

$$\% I = 100(R_{Hb} - R_{Hi})/R_{Hb} \quad (4)$$

where R_{Hb} and R_{Hi} are the hydrogen evolution rates in the absence and presence of PIP respectively.

2.5. Computational Details

Among quantum chemical methods, the DFT has some advantage since its calculation time is roughly the same as a Hartree–Fock procedure that includes the relativistic effect as an electron correlation term. The hybrid version of DFT and Hartree–Fock (HF) methods, i.e., B3LYP, which incorporates a Becke's 3- parameter functional (B3) as well as a mixture of HF with DFT ex-change terms associated with the gradient-corrected correlation functional of Lee et al. 1988 [9] was used in this study to carryout quantum calculations using Jaguar, a calculation package from Schrodinger LLC, New York, NY, 2009.

3. Results and Discussion

3.1. Corrosion rate and Inhibition Efficiency

The weight loss of mild steel in 0.5 M H_2SO_4 solution in the absence and presence of different concentrations of PIP was determined at 300 – 333 K. Figure 2 shows the weight loss - time curves for mild steel corrosion in 0.5 M H_2SO_4

without and with different concentrations of PIP at (a) 303 K (b) 313 K (c) 323 K (d) 333 K.

Inspection of the figures shows that weight loss of the metal varies linearly with immersion time and was reduced in the presence of the inhibitor compared to that of the free acid solution. It was also observed that weight loss increases with increase in temperature with greater weight losses obtained at 333 K.

The values of the corrosion rates and inhibition efficiencies computed using equations (1-4) respectively are shown in table 1 for both weight loss (a) and hydrogen evolution (b) methods. It is clearly seen from the table that the corrosion rates were reduced in the presence of PIP compared to its absence and increased with increase in temperature both in the absence and presence of the inhibitor. The corrosion rate values are also seen to decrease with increase in concentration of PIP (Fig 3). This actually confirms that the addition of even a very small amount (0.00001 M) of PIP to the acid solution retards the corrosion rate of the metal and the extent of retardation is concentration and temperature dependent. The values obtained from gravimetric and gasometric measurements were comparative, therefore, only values obtained by weight loss technique were used for further computations and graphical analyses.

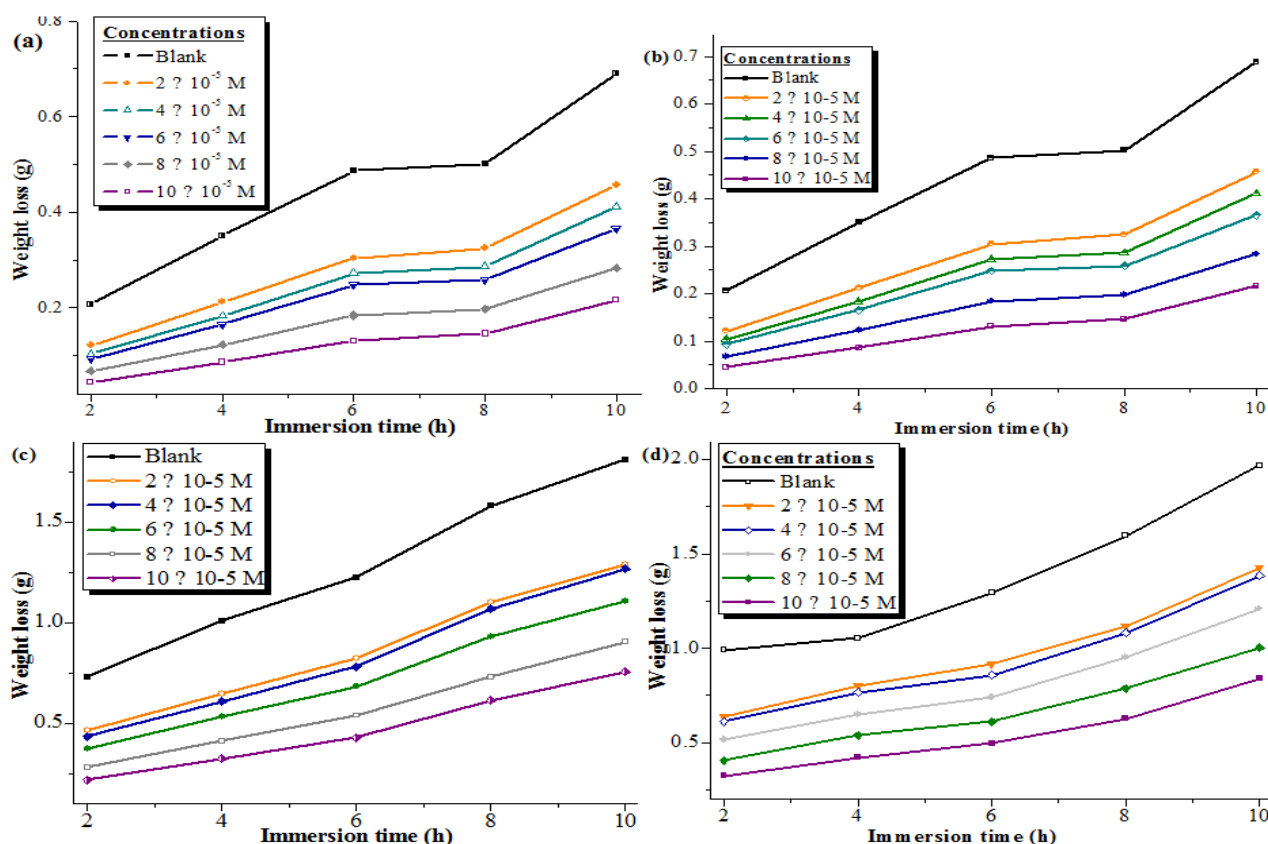


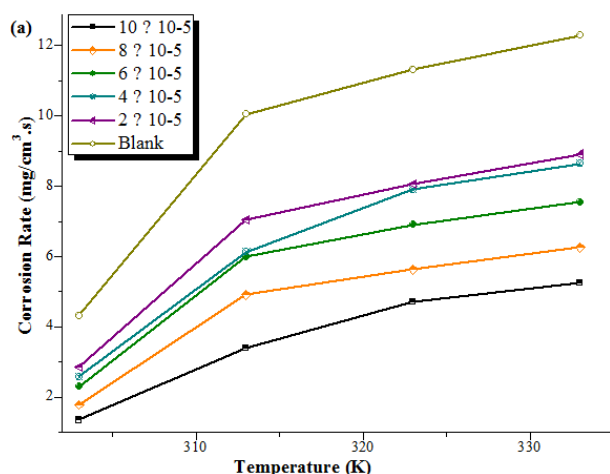
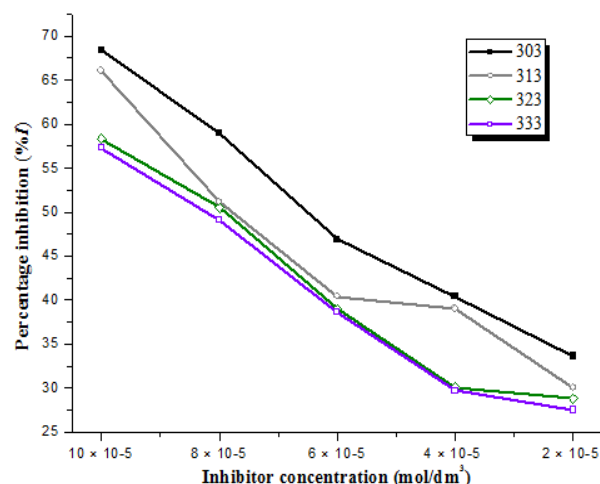
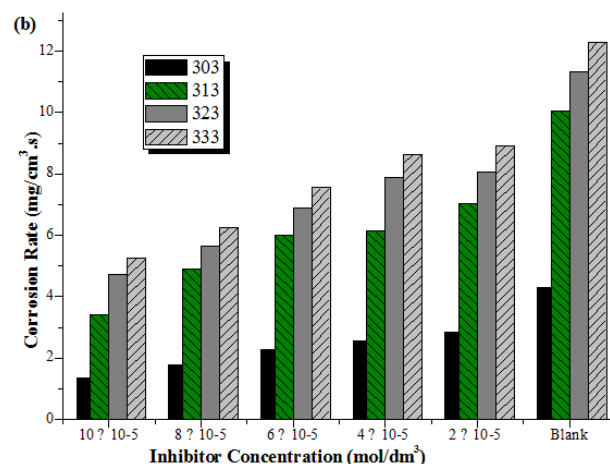
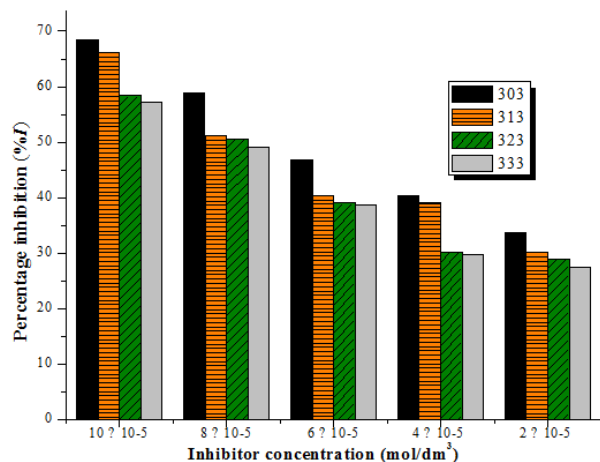
Fig 2. Weight loss – time curves for the inhibition of mild steel corrosion in 0.5 M H_2SO_4 in the absence and presence of different concentrations of PIP at (a) 303 K (b) 313 K (c) 323 K (d) 333 K

Table 1(a). Calculated values of corrosion rate (v) and inhibition efficiency (%I) for the inhibition of mild steel corrosion in 0.5 M H_2SO_4 in the absence and presence of different concentrations of PIP at 303 – 333 K using weight loss measurement.

Conc (M)	303K		313K		323K		333K	
	v	% I	v	% I	v	% I	v	% I
Blank	4.31	-	10.05	-	11.31	-	12.29	-
10×10^{-5}	1.34	68.45	3.40	66.10	4.71	58.36	5.25	57.28
8×10^{-5}	1.77	58.93	4.91	51.14	5.63	50.48	6.26	49.06
6×10^{-5}	2.29	46.87	5.99	40.40	6.90	38.99	7.55	38.57
4×10^{-5}	2.57	40.37	6.13	39.00	7.90	30.06	8.64	29.70
2×10^{-5}	2.86	33.64	7.03	30.05	8.05	28.82	8.91	27.50

Table (b). Calculated values of corrosion rate (v) and inhibition efficiency (%I) for the inhibition of mild steel corrosion in 0.5 M H_2SO_4 in the absence and presence of different concentrations of PIP at 303 – 333 K using hydrogen evolution measurement.

Conc (M)	303K		313K		323K		333K	
	v	% I	v	% I	v	% I	v	% I
Blank	4.30	-	10.03	-	11.30	-	12.28	-
10×10^{-5}	1.67	61.3	4.29	57.3	5.20	54.0	6.16	49.9
8×10^{-5}	2.02	53.2	5.08	49.5	6.10	46.1	6.98	43.2
6×10^{-5}	2.41	44.1	5.99	40.3	7.06	37.6	8.12	33.9
4×10^{-5}	2.57	40.3	6.25	37.8	7.45	34.1	8.42	31.5
2×10^{-5}	2.80	35.1	6.68	33.2	7.89	30.2	8.92	27.4

**Fig 3 (a).** Corrosion rate - temperature curve for the inhibition of mild steel corrosion in 0.5 M H_2SO_4 in the absence and presence of different concentrations of PIP**Fig 4 (a).** A plot of inhibition efficiency (%) against concentration of PIP at different temperatures for the inhibition of mild steel corrosion in 0.5 M H_2SO_4 solution.**Fig 3 (b).** Variation of corrosion rate with temperature for the inhibition of mild steel corrosion in 0.5 M H_2SO_4 in the absence and presence of different concentrations of PIP**Fig 4 (b).** Variation of inhibition efficiency (%) with concentration of PIP at different temperatures for the inhibition of mild steel corrosion in 0.5 M H_2SO_4 in the absence and presence of different concentrations of PIP.

The table also shows that inhibition efficiency increases with increase in concentration but decreases with increase in temperature. The maximum inhibition efficiency of 68.45% and 33.64% were obtained for 10×10^{-5} M PIP at 303 and 333K respectively. PIP contains heteroatoms O and N as well as multiple bonds and aromatic rings in its molecular structure. The inhibition of mild steel corrosion in the acid medium may be attributed to adsorption of PIP components through these atoms, which are regarded as adsorption centers, on to the metal surface. It is difficult at this stage to assign inhibitive effect to a particular constituent. Further investigation using surface analytical techniques or functional group spectrophotometric studies on the corrosion products may enable the characterization of the active materials in the adsorbed layer and to assist in identifying the most active ingredient.

The observed decrease in % I with increase in temperature suggests that PIP was physically adsorbed on to the mild steel surface. Physical adsorption is associated with weak electrostatic interactions between charged molecule and charged metal and may be facilitated by the presence of vacant d-orbitals in the iron that makes up the mild steel. The adsorption of the inhibitor at the metal-solution interface is generally assumed to be the first step in the action mechanism of corrosion inhibition in an aggressive acid medium. However, for a given inhibitor, the mechanism of adsorption depends on some factors such as the nature of the metal and the corrosive medium, the pH and the concentration of the inhibitor as well as the type and nature of the functional group present in the inhibitor system since different groups adsorb to different extents [10]. A decrease in % I with temperature has been reported by Olivares *et al* [11] to be due to a reduction in stability of the adsorbed film at higher temperature: as temperature increases, Gibbs free energy and enthalpy rises to a higher value, so that some of the chemical bonds joining the molecules on to the metallic surface are impaired, and the stability of the film reduces. This is likely to result in desorption of the inhibitor film from the metal surface and a shift in the position of the inhibitor-metal interfacial equilibrium.

3.2. Adsorption Studies

An organic compound may be considered efficient and a successful inhibitor of acid corrosion if it is able to get adsorbed on the metal surface and this involves the replacement of the water molecules at the corroding interface. Assuming that the metal is corroding uniformly, the corrosion rate of the acid in the absence of the inhibitor is representative of the total number of available corroding sites. Therefore, the corrosion rate in the presence of the inhibitor may be taken as representative of the number of potentially corroding sites that remain after blockage due to inhibitor adsorption [11]. Assuming a direct relationship between the % I and the degree of surface coverage (θ) given in equation (5), the adsorption characteristics of PIP in 0.5M H_2SO_4 solutions may be determined.

$$\% I = 100 \theta \quad (5)$$

To ascertain the nature of adsorption, the surface coverage data for PIP at 303-333 K were theoretically fitted into different adsorption models and the correlation coefficients (R^2) were used to determine the best fit, which was obtained with Temkin adsorption isotherm. According to Temkin adsorption model, the adsorption of charged molecules on a charged heterogeneous surface is given by the relationship:

$$\exp(-2a\theta) = KC \quad (6)$$

Where “ a ” is the molecular interaction parameter, θ is the degree of surface coverage; K is the equilibrium constant of adsorption and C is the concentration of inhibitor. The relationship between K and free energy of adsorption (ΔG^*_{ads}) is given by

$$K = 0.018 \exp(-\Delta G^*_{ads}/RT) \quad (7)$$

where 0.018 is the reciprocal of 55.5 which represents the concentration of water and T is the absolute temperature. Thus, a plot of surface coverage (θ) against the logarithm of PIP concentration at different temperatures yields linear plots depicted in figure 5 with R^2 values greater than 0.7498, and substantially indicating that the adsorption process maybe best described by Temkin adsorption model. Table 2 shows the adsorption parameters deduced from the Temkin isotherm. The values of “ a ” in all cases are negative indicating that repulsion exists in the adsorption layer. The equilibrium constant of adsorption, K , is a parameter associated with the strength of interaction in the adsorbed layer. The decrease in K values with increasing temperature suggests that the metal-inhibitor binding strength weakens as temperature increases (suggesting possible desorption of the inhibitor molecules) and this trend indicates that the inhibitor is physically adsorbed on the mild steel surface. The negative ΔG^*_{ads} values obtained indicate the spontaneous nature of the adsorption process.

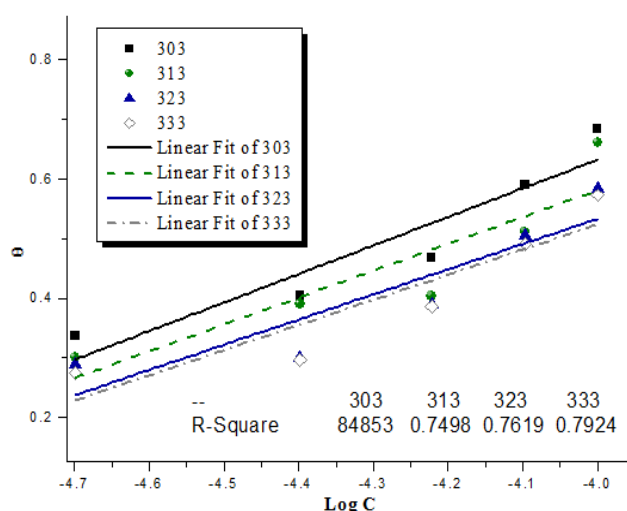
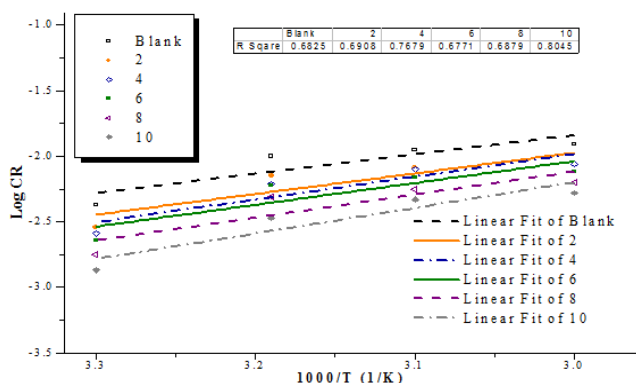


Fig 5. Temkin adsorption isotherm for the inhibition of mild steel corrosion in 0.5 M H_2SO_4 solution containing different concentration of PIP at different temperatures.

Table 2. Adsorption parameters obtained from Temkin adsorption isotherm for the inhibition of mild steel corrosion in 0.5 M H₂SO₄ in the presence of PIP.

Temp(K)	K _{ads} (J/mol ⁻¹)	-ΔG _{ads} (kJ/mol)	a
303	502.51	25.79	-26.47
313	240.41	27.72	-27.42
323	191.45	24.90	-29.53
333	151.18	25.01	-29.53

3.3. Kinetic/ Thermodynamic Considerations

**Fig 6.** Arrhenius plot for the inhibition of mild steel corrosion in 0.5 M

The calculated corrosion rate data at the different temperatures studied were fit into the Arrhenius equation, which describes the dependence of the rate of a reaction on temperature. The linearized form of the equation is given by

$$\log v = \log A - E_a/2.303RT \quad (8)$$

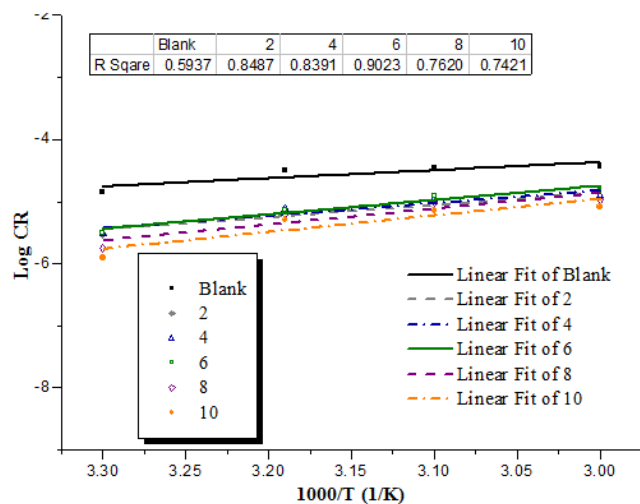
where v is the corrosion rate, A is the Arrhenius pre-exponential constant, R is the molar gas constant, and T is the absolute temperature. A plot of $\log v$ against $1/T$ produces straight lines shown (fig 6), with slope as $-E_a/2.303R$ and intercept as $\log A$ activation parameters calculated from the plot are displayed in table 3. The transition state equation (9) afforded thermodynamic parameters (table 3) such as enthalpy, ΔH^*_{ads} and entropy ΔS^*_{ads} from a plot of $\log v/T$ against $1/T$ shown in Fig 6.

$$v = RT/Nh \exp(\Delta S^*_{ads}/R) \exp(\Delta H^*_{ads}/RT) \quad (9)$$

where N is the Avogadro's number and h is the planks constant. The enthalpy was calculated from the slope ($-\Delta H^*_{ads}/R$) while the entropy was calculated from the intercept $\{\ln(R/Nh) + (\Delta S^*_{ads}/R)\}$ of the plot. From table 3, it is seen that E_a is lowest for the free acid solution but higher in the

presence of the inhibitor, with E_a values increasing as the concentration of the inhibitor increases. The increase in E_a with concentration is associated with an increase in energy barrier for the mild steel corrosion, and is dependent on the concentration of the inhibitor. The value of ΔH^*_{ads} obtained were all positive, indicating the endothermic nature of the corrosion process. The mode of adsorption is based on the absolute value of ΔH^*_{ads} [12]. Generally, enthalpy values lower than 41.86 kJ/mol indicate physical adsorption while values approaching 100 kJ/mol indicate chemical adsorption [13]. The absolute enthalpy values obtained in this study are consistent with physisorption mechanism for all concentrations of PIP and temperatures.

The entropy of adsorption ΔS^*_{ads} (table 3) obtained are all negative indicating that the adsorption process is accompanied by a decrease in chaos for all the systems studied due to adsorption of components of PIP on the metal surface [14]. This decrease in entropy of adsorption has been explained by Ituen and Udo [15] to be associated with the drift of the inhibitor molecules from the solution to the metal-solution interface resulting in a decrease in the number of moles of the PIP in the bulk solution, hence decreased solution entropy. It may also be inferred from the negative entropy values that there is orderliness in the adsorbed layer [16]. The ΔG^*_{ads} obtained are also negative, and more negative than -20 kJ/mol, a condition that confirms physisorption mechanism earlier proposed, so far not more negative than -40 kJ/mol.

**Fig 7.** Transition state plot for the corrosion of mild steel in 0.5 M H₂SO₄ solution containing different concentration of PIP**Table 3.** Activation and thermodynamic parameters deduced from Arrhenius and transition state plot for the inhibition of mild steel corrosion in 0.5 M H₂SO₄ in the absence and presence different concentrations of PIP.

Concentration	E _a (J/mol)	A x 10 ⁻³	-ΔS* (J/mol)	ΔH* (J/mol)
Blank	2.74	3.54	104.15	1.33
2 x 10 ⁻⁵	2.93	2.57	100.51	1.48
4 x 10 ⁻⁵	3.26	2.16	99.36	1.59
6 x 10 ⁻⁵	3.10	2.04	98.79	1.54
8 x 10 ⁻⁵	3.27	1.57	95.42	1.65
10 x 10 ⁻⁵	3.27	1.57	93.62	1.83

3.4. Uv-Visible Spectroscopic Analysis

The inhibition of mild steel corrosion in 0.5 M sulphuric acid by different concentrations of PIP was investigated using uv-vis technique. Data obtained shows that there was a shift in wavelength of absorption to higher wavelengths. This suggests the possibility of strong interaction between the PIP molecules and the metal surface, hence its inhibitive effect. The uv-vis spectrum showing the changes in absorbance for freshly prepared PIP and PIP with the mild steel after three days immersion is depicted in figure 8 below

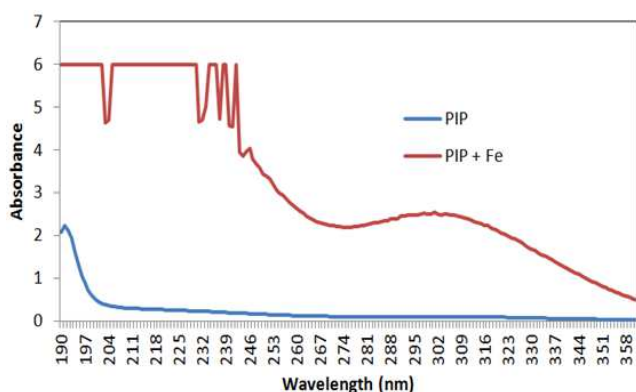


Fig 8. Uv-visible spectrum showing the changes in absorbance for freshly prepared PIP and PIP with the mild steel after three days immersion

3.5. Quantum Chemical Studies

Tables 4 and 5 show some quantum chemical parameters and Mullikan charge distribution while Figs. 8-11 show the optimized geometry, the HOMO density distribution, the LUMO density distribution and the Mullikan charge population analysis plots respectively for PIP molecule in aqueous phase obtained with DFT at the B3LYP/6-31G basis set in aqueous phase of Jaguar version 4.4 programme (Schrodinger LLC, New York, NY, 2009). The relationship between inhibition efficiency of corrosion inhibitors and molecular parameters like E_{HOMO} , E_{LUMO} and ΔE were investigated to obtain some useful information on the reactivity of the molecule since the reactive ability of the inhibitor is closely related to its frontier molecular orbitals, the HOMO and the LUMO [4]. The HOMO is usually the region of electron density hence it is associated with the electron donating ability of the molecule while the LUMO is

associated with the electron accepting ability of the molecule. It is well established in literature that the higher the HOMO energy (E_{HOMO}) of the inhibitor, the greater its ability to donate electrons to unoccupied d-orbital of the metal and the higher the corrosion inhibition efficiency.

Table 4. Some molecular properties of PIP calculated using DFT at the B3LYP/6-31G basis set in aqueous phase.

Molecular Parameter	Calculated value (eV)
E_{HOMO}	- 4.97
E_{LUMO}	- 0.98
ΔE	3.99
Total energy	- 35590.60
Point group	C_1

From table 4, it is evident that PIP has a high E_{HOMO} suggesting that the interaction between PIP and mild steel is electrostatic in nature (i.e. physisorption) hence confirming the result obtained experimentally. This also indicates that the adsorption of the inhibitor is facilitated, thereby, ensuring an improved transport process through the adsorbed layer and better inhibition efficiency [4]. The energy gap (ΔE) that is the difference between the E_{LUMO} and E_{HOMO} is an important stability index and also another parameter found to have excellent correlations with inhibition efficiencies. It is equally related to hardness or softness of a molecule. Soft molecules are more reactive than hard molecules because the energy to remove electron from the last occupied orbital will be low [17-18]. Low value of ΔE indicates better inhibition efficiency. Based on the result in Table 4, the low value of ΔE implies good inhibition efficiency; as the excitation energy to remove electron from the last occupied orbital will be low [19]. It also suggests that the molecule PIP could be more polarized, of high chemical reactivity, low kinetic stability and hence termed a soft molecule [20-21].

The Mullikan charge distribution of PIP is presented in table 5. Literature reports that the more negative the atomic charges of the adsorbed center, the more easily the atom donates its electron to the unoccupied orbital of the metal [22]. From the result in Figs 8-10 show that Nitrogen, Oxygen and some carbon atoms have large negative charges suggesting that these active centres with excess charges could act as nucleophilic reagents as earlier reported [4].

Table 5. Mullikan charge distribution of PIP

Atom Charge	N1-0.619	C20.432	N3-0.525	C4 0.138	C5 0.037	C6-0.015	C7-0.014	C8 0.047	C9 0.185	C10 -0.133
	C11-0.163	C12-0.144	C13-0.148	H14 0.124	H15 0.143	C16-0.153	C17-0.135	C18-0.147	C19-0.147	H20 0.132
	H21 0.138	C22 0.268	C23 0.088	C24-0.267	C25 0.155	C26-0.222	C27-0.054	H28 0.188	O29-0.659	H30 0.366
	H31 0.135	H32 0.162	H33 0.134	H34 0.143	H35 0.135	C36-0.456	C37 0.0047	C38-0.458	C39-0.457	H40 0.153
	H41 0.144	H42 0.153	H430.136	H44 0.163	H45 0.149	H46 0.136	H47 0.148	H48 0.163	C49-0.456	C50 0.032
	C51-0.439	C52-0.439	H53 .151	H54 0.138	H55 0.151	H56 0.137	H57 0.138	H58 0.138	H59 0.137	H60 0.138
	H61 0.148	H62 0.423								

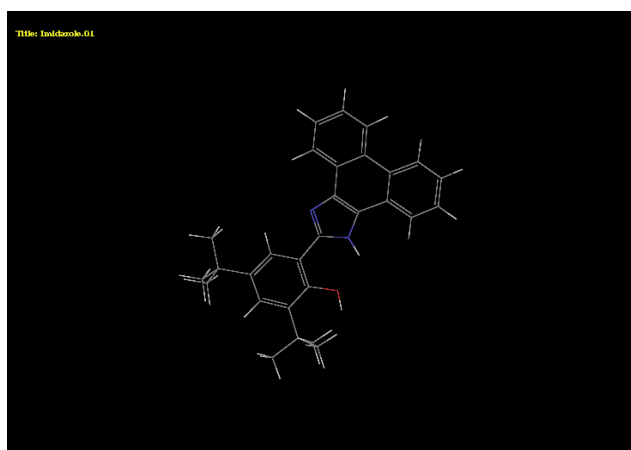


Fig 9. Optimized PIP structure

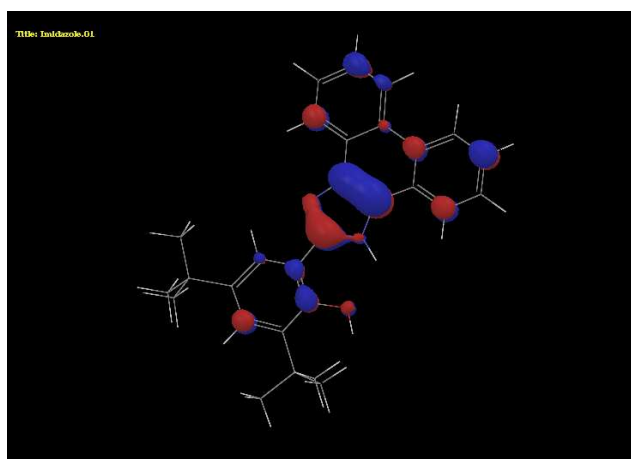


Fig 10. The highest occupied molecular orbital (HOMO) density of PIP using DFT at the B3LYP/6-31G* basis set level.

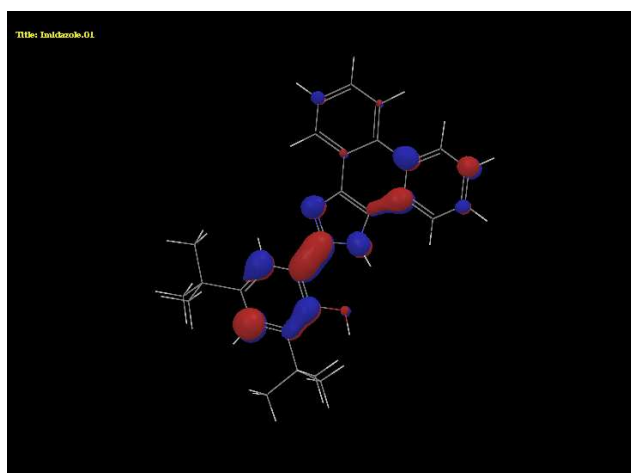


Fig 11. The lowest unoccupied molecular orbital (LUMO) density of PIP using DFT at the B3LYP/6-31G* basis set level.

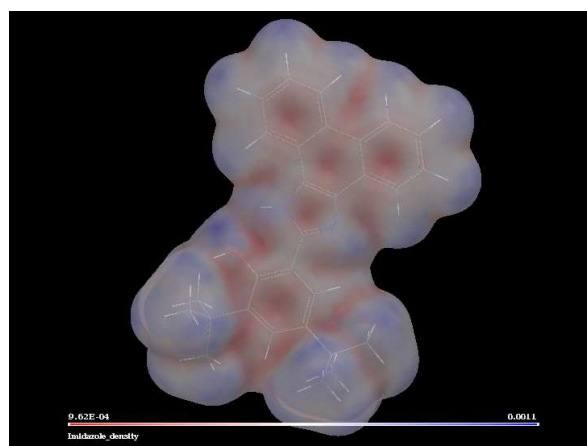


Fig 12. Total electron density diagram of PIP [the electron rich region is red and the electron poor region is blue for the PIP neutral molecule]

4. Conclusion

On the basis of this study, the following conclusions have been drawn:

- The inhibitor (PIP) acts as an effective and efficient inhibitor for mild steel corrosion in sulphuric acid medium at all temperatures studied, being a better inhibitor at 303 K
- Corrosion rate increases as temperature increases both in the absence and presence of the inhibitor and decreases further in the presence of the inhibitor.
- Inhibition efficiency of PIP increases with increase in concentration of PIP but decreases with increase in temperature
- The corrosion inhibition is probably due to the adsorption of the inhibitor on to the mild steel surface and thus blocking the corrosion active sites by the physical adsorption mechanism
- The inhibition of mild steel corrosion by PIP obeys Temkin adsorption model at all the concentrations and temperatures studied
- The values of entropy of adsorption obtained are low, indicating spontaneous adsorption and the instability of the adsorbed layer
- The adsorption process is endothermic as implicated by the values of the enthalpy of adsorption and there is repulsion in the adsorbed layer from the values of “*a*” obtained.
- Data obtained from quantum chemical calculations using DFT at B3LYP/6-31G basis set correlated to the inhibitive effect of PIP.
- PIP is a recommended and green corrosion inhibitor for industries.

Acknowledgements

The authors wish to acknowledge the Department of Chemistry, University of Uyo, Nigeria, for providing the

facilities for the experimental section, Denmark Technical University for the facilities for the computational section and one of the authors, Dr. A.O. Eseola for the newly synthesized inhibitor used in this research.

References

- [1] Brown, E. E. Kluwer Academic Press, New York. 1998
- [2] Talati, J. D. and Gandhi D. K. Corros. Sci. 2003, 23 (12): 1315 – 1332
- [3] Umoren, S. A., Obot, I. B., Ebenso, E. E., Obi- Egbedi, N. Portuga. Electrochim. acta. 2008, 26: 199-209
- [4] N.O. Obi-Egbedi, and I.B.Obot. Arab. Journ. Chem. 2010, 5 (1): 121-133
- [5] Eseola, A. O.; Li, W.; Sun, W. H.; Zhang, M.; Xiao, L.; Woods, J. A. O. Dyes & Pigmen. 2011, 88: 262-273.
- [6] Umoren, S. A., Solomon, M. M., Udousoro, I. I., Udoh, A.P. Cellulos. 2010, 17: 635-648.
- [7] Umoren, S. A. Cellulos. 2008 (a), 15: 751–761.
- [8] Umoren, S. A., Ekanem, U. F. Chem. Eng. Commun. 2010, 197: 1339-1356.
- [9] E. Jamalizadeh, S.M.A. Hosseini and A.H. Jafari. Corros. Sci. 2009, 51: 1428–1435
- [10] Oguzie, E. E. Mater Chem Phys. 2006, 99 (2/3): 441-446.
- [11] Olivares, O., Likhanova, N. V., Gomez, B., Navearreie, J., Llanoserrano M. E., Arce, E., Hallen, J. M.. Appl. Surf. Sci. 2006, 252: 2894-2909.
- [12] Umoren, S. A. Cellulos. 2008 (b), 15: 751–761.
- [13] Martinez, S. and Stern, I. J. Appli. Electrochem. 2001, 31 (9): 973-978.
- [14] El-Etre, A. Y. Corros. Sci. 2003, 45 (11): 2485-2495.
- [15] Ituen, E. B. and Udo, U. E. Der Chimic. Act. 2012, 3 (6): 1394-1405
- [16] Ituen, E. B., Odozi, N. W., Udo, U.E., Dan, E. U. IOSR-J. Appli. Chem. 2013, 3 (4): 52-59
- [17] Bentiss, F., Traisnel M., Chaibi N, Mernari B, Vezin H, Lagrennee M. Corros. Sci. 44 2002, (10): 2271-2289.
- [18] Umoren, S. A., Ogbobe, O., Igwe, I. O., Ebenso, E. E. Corros. Sci. 2008, 50: 1998-2006.
- [19] Gece, G. Corros. Sci. 2008, 50: 2981
- [20] Dwivedi, A., Misra, N. Der. Pharma. Chem. 2010, 2: 58 - 65.
- [21] N.O. Obi-Egbedi, K.E. Essien, I.B.Obot. J. Comput. Method Mol. Design, 2011, 1(1): 26-43
- [22] Xia, S., Qiu, M., Yu, L., Lui, F., Zhao, H. Corrs. Sci. 2008, 50 :2021-2029